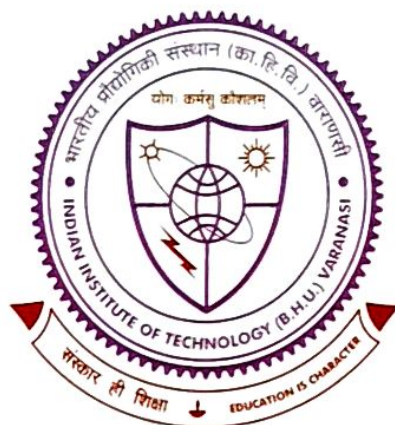


Carbon Materials and their Composites for Device Applications



Thesis submitted in partial fulfillment for the
Award of Degree

Doctor of Philosophy

By

Nikhil

SCHOOL OF MATERIALS SCIENCE & TECHNOLOGY
INDIAN INSTITUTE OF TECHNOLOGY
(BANARAS HINDU UNIVERSITY)
VARANASI- 221005
INDIA

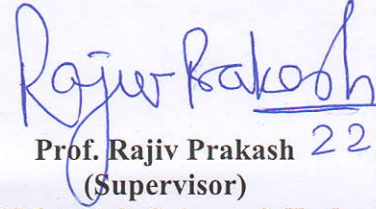
Roll No. 16111007

2022

CERTIFICATE

It is certified that the work contained in the thesis titled "Carbon Materials and their Composites for Device Applications" by "*Nikhil*" has been carried out under my supervision and that this work has not been submitted elsewhere for a degree.

It is further certified that the student has fulfilled all the requirements of Comprehensive, Candidacy and SOTA.


Prof. Rajiv Prakash 22/7/2022
(Supervisor)

School of Materials Science & Technology,
Indian Institute of Technology,
Banaras Hindu University,
Varanasi-221005

Professor/आचार्य

School of Materials Science & Technology/पदार्थ विज्ञान एवं प्रौद्योगिकी स्कूल
Indian Institute of Technology/भारतीय प्रौद्योगिकी संस्थान
(Banaras Hindu University), Varanasi/काशी हिन्दू विश्वविद्यालय, वाराणसी

DECLARATION BY THE CANDIDATE

I, *Nikhil*, certify that the work embodied in this thesis is my own bonafide work and carried out by me under the supervision of *Prof. Rajiv Prakash* from **July 2016 to June 2022** at the *School of Materials Science & Technology*, Indian Institute of Technology, Banaras Hindu University, Varanasi. The matter embodied in this thesis has not been submitted for the award of any other degree/diploma. I declare that I have faithfully acknowledged and given credits to the research workers wherever their works have been cited in my work in this thesis. I further declare that I have not willfully copied any other's work, paragraphs, text, data, results, etc., reported in journals, books, magazines, reports, dissertations, theses, etc., or available at websites and have not included them in this thesis and have not cited as my own work.

Date: 22-7-2022
Place: Varanasi

Nikhil
(Nikhil)

Certificate by the Supervisor

It is certified that the above statement made by the student is correct to the best of my knowledge.

Rajiv Prakash
Prof. Rajiv Prakash

Supervisor

Professor/आचार्य

School of Materials Science & Technology/पदार्थ विज्ञान एवं प्रौद्योगिकी स्कूल
Indian Institute of Technology/भारतीय प्रौद्योगिकी संस्थान
(Banaras Hindu University), Varanasi/काशी हिन्दू विश्वविद्यालय, वाराणसी

Rajiv Prakash
Coordinator 22/7/2022
Coordinator/समन्वयक

School of Materials Science & Technology/पदार्थ विज्ञान एवं प्रौद्योगिकी स्कूल
Indian Institute of Technology/भारतीय प्रौद्योगिकी संस्थान
(Banaras Hindu University), Varanasi/काशी हिन्दू विश्वविद्यालय, वाराणसी

COPYRIGHT TRANSFER CERTIFICATE

Title of the Thesis: Carbon Materials and their Composites for Device Applications

Name of the Student: NIKHIL

Copyright Transfer

The undersigned hereby assigns to the Indian Institute of Technology (Banaras Hindu University) Varanasi all rights under copyright that may exist in and for the above thesis submitted for the award of the "Doctor of Philosophy".

Date: 22-7-2022

Place: Varanasi

Nikhil
Signature of student

(NIKHIL)

Note: However, the author may reproduce or authorize others to reproduce material extracted verbatim from the thesis or derivative of the thesis for author's personal use provided that the source and the Institute's copyright notice are indicated.

Acknowledgement

The work presented in this thesis would not have been possible without my close association with many peoples who were always there when I needed them the most. I take this opportunity to acknowledge them and extend my sincere gratitude for helping me make this thesis a possibility. At this moment of accomplishment, first of all I would like to pay the homage to the founder of Banaras Hindu University, Pandit Madan Mohan Malvia ji, who made this glorious temple to realize spiritual, technical and scientific knowledge about this vast existing universe.

*I embrace the opportunity to express my deep sense of gratitude to my supervisor **Dr. Rajiv Prakash**, Professor, School of Materials Science & Technology, IIT (B.H.U.), Varanasi for his constant guidance, valuable suggestions and kind encouragement during my association with his research group. His encouragement, constant support, intellectual stimulation, perceptive guidance, immensely valuable ideas, and suggestions from the initial to the final level enabled me to develop an understanding of the subject. His scholarly suggestions, prudent admonitions, immense interest, constant help and affectionate behavior have been a source of inspiration for me. His suggestions will remain with me as an inexhaustible source of scientific learning throughout my life.*

*I would like to express my sincere and whole hearted gratitude to **Prof. P. Maiti, Dr. A. K. Singh, Dr. C. Rath, Dr. C. Upadhyay, Dr. B. N. Pal, Dr. Ashish kumar Mishra, Dr. Sanjay Singh Dr. Shravan kumar Mishra. And Dr. Nikhil** (School of Materials Science and Technology, IIT-BHU, Varanasi) for discussion during seminars and valuable suggestions given by them. I am indeed obliged and sincerely thankful to my RPEC member **Dr.Indrajeet Sinha**, Department of Chemistry, IIT- BHU for his guidance and untiring attention right from the inception to the successful completion of assigned research work. Most of the results described in this thesis would not have been obtained without a close collaboration with few laboratories..*

Acknowledgement

I am thankful to the unknown reviewers who have rejected my papers several times in some of the international conferences and journals. The comments that they provided helped to polish our articles in better shape. But the bigger and nobler cause of thanking them is that the rejections have equipped me with high level of patience and helped me a lot to exercise/implement my spiritual thoughts in practice.

*My acknowledgement will never be complete without the special mention of my lab seniors who have taught me the lab culture and have lived by example to make me understand the hard facts of life. I would like to acknowledge , **Dr. Gopal Ji, Dr. Monika Srivastava, Dr. Rajiv kumar Pandey, Dr. Arun K. Singh, Dr. Akhilesh K. Singh, Dr. Ashish Kumar, Dr. Uday Pratap Azad, Dr. Narsingh Raw Nirala, Dr. Neeraj Giri, Dr. Madhu Tiwari, Dr. Kashish, Dr. Preeti Tiwari, Dr. Chandrajeet verma, Dr. Vinita, Dr. Richa Mishra , Dr. Manish Kumar Singh** for all their support and motivation during the initial days of my PhD. I can see my thesis in the good shape because of his help in formatting the entire thesis. I express my special thanks to my senior **Dr. Praveen Kumar Sahu** for his guidance, support, motivation and valuable suggestions. Also I am thankful to my lab fellows and juniors of my lab specially **Ankit Verma, Saurabh ,Radhe Shyam, , Ravi , Vineet, Aniruddha, Shweta, Priya, Nupur, Ajay ,Rajpal, Shubhajit**, for their helping behavior. I am also thankful to all, to whom I could not mention here who helped me directly or indirectly throughout the work. I am thankful to all non-teaching staff of SMST, IIT (BHU) and CIFIC for their cooperation at all levels.*

*I express my indebtedness to my parents **Smt. Kiran Bala and Sri. Raj Bahadur**, my sisters **Dimple, Pooja** for their love, affection and support during every moment in my life.*

I gratefully acknowledge the MHRD and CSIR New Delhi for providing me the necessary funding and fellowship to pursue research work.

(Nikhil)

		Page No.
List of Figures		i-v
List of Tables		vi
List of Abbreviations / Symbols		vii-ix
Abstract		x
Chapter – 1	Introduction & Literature Survey	1-44
	1.1 Introduction	1
	1.2 Dimensional categorization of nanomaterials	1
	1.3 Brief history of Carbon and Carbon Nanomaterials	2
	1.4 Applications of Carbon Nanomaterials and their Composites	10
	1.5 Motivation and Objective of the thesis	39
	1.6 Organization of the thesis	40
Chapter – 2	Experimental and Characterization Techniques	45-78
	2.1 Experimental and Characterization Techniques	45
Chapter – 3	Self-assembled polythiophene/graphene oxide nanocomposite thin film at air-liquid interface in polymer thin film transistors	79-98
	3.1 Introduction	79
	3.2 Results and Discussion	80
	3.2 Conclusions	98
Chapter – 4	Self-assembled thin film of thienothiophene polymer-reduced graphene oxide nano-composite at air-liquid interface in organic field effect transistor fabrication	99-116
	4.1 Introduction	99
	4.2 Results and Discussion	101
	4.3 Conclusions	115
Chapter – 5	Poly(2,5-bis(3-alkylthiophen-2-yl)thieno[3,2-b]thiophene)-Graphene quantum dots nanocomposite floating film at air-liquid interface in organic thin-film transistor application	117-130
	5.1 Introduction	117
	5.3 Results and Discussion	119
	5.4 Conclusions	130

Chapter – 6	Application of natural biomass-derived two-dimensional carbon material for arsenic sensing	131-146
	6.1 Introduction	131
	6.2 Results and Discussion	133
	6.3 Conclusions	145
Chapter – 7	Summary and Conclusion	147-153
References		154-191
List of Publications		

List of figures

Figure No.	Figure Caption	Page No.
Figure 1.1	Carbon allotropes with different dimensions	2
Figure 1.2	Graphite's crystal structure	4
Figure 1.3	Schematic diagram showing how a hexagonal sheet of graphite is 'rolled' to form a carbon nanotube	6
Figure 1.4	Depiction of the atomic structure of (a) an armchair and (b) a zig-zag nanotube	6
Figure 1.5	(a) Illustrations of the graphene crystal structure, Brillouin zone, electronic dispersion spectrum, and (b) "Rippled graphene" simulation using a Monte Carlo method. The length of the red arrows is around 8 nm.	8
Figure 1.6	Log scale diameter comparison of fibrous carbon compounds	9
Figure 1.7	Band structure illustration of a polymeric chain in case of (a) ionization process (b)The formation of a polaron.	13
Figure 1.8	A polymer chain's band structure: (a) two polarons; (b) one bipolaron	14
Figure 1.9	Top: schematic illustration of the geometric structure of a neutral soliton on a trans-polyacetylene chain. Bottom: bandstructure for a trans-polyacetylene chain containing (a) a neutral soliton, (b) a positively charged soliton, and (c) a negatively charged soliton	15
Figure 1.10	Edge on (a) face on (b) and, Flat-on (c) orientation of regioregular PTs	17
Figure 1.11	Charge transport in OFET fabricated using (a) edge-on oriented and (b) face-on oriented polymer chains.	18
Figure 1.12	Schematic depiction of the working principle of a chemical (biochemical) sensor	23
Figure 1.13	A working electrode (WE), a counter electrode (CE), and a reference electrode comprise an electrochemical system (RE)	24
Figure 1.14	Operating principle of an electrochemical sensor	25
Figure 2.1	Schematic of GO transfer from the aqueous phase to the chloroform phase	48
Figure 2.2	Schematic of PBTTT/GO or rGO or GQDs nanocomposite FTM film formation	49
Figure 2.3	Activated carbon in two dimensions(2D) is depicted graphically	51
Figure 2.4	Vacuum thermal evaporation unit (Hind HIVAC" model No-12A4D, India).	53
Figure 2.5	Oxidation furnace (model no. MB71, Thermco Inc., USA)	54
Figure 2.6	Electric Oven	55
Figure 2.7	Semiconductor parameter analyzer	56

List of figures

Figure 2.8	The basic instrumentation of UV-Vis spectrophotometer	57
Figure 2.9	The basic instrumentation of the FT-IR spectrometer	58
Figure 2.10	Raman principle	59
Figure 2.11	Schematic representation of experimental setup in Cyclic voltammetry	61
Figure 2.12	Schematic representation of basic components of SEM	62
Figure 2.13	Schematic representation of basic components of TEM	63
Figure 2.14	Schematic representation of tapping mode in AFM	65
Figure 2.15	Schematic representation of X-ray diffraction	66
Figure 2.16	BET Surface Area Analyzer	67
Figure 2.17	Configurations of OTFT-based device geometries (a) bottom-gate top contact, (b) bottom gate bottom contact, (c) top gate bottom contact, (d) top gate top contact	72
Figure 2.18	The illustration depicts three scenarios for a p-type semiconductor in an OFET: (a) The flat-band condition when no bias is applied. (b) Accumulation regime when the metal is subjected to a negative bias (c) Depletion regime in which the metal is biased positively	74
Figure 2.19	(a) An organic TFT's energy level diagram at $V_G=0$ and $V_D=0$. (b-e) show the field effect transistor operation principle for (b) electron accumulation and (d) transport and (c) hole accumulation and (e) transport	76
Figure 3.1	(a) SEM and (b) TEM images of the as-synthesized GO. (c) XRD pattern of the GO powder. Inset shows the SAED pattern of the as-synthesised GO powder. (d) UV-vis spectrum (inset shows the FT-IR spectrum), and (e) Schematic structure of the GO sheet. (f) Raman spectrum of GO when excited using a 532 nm laser source	84
Figure 3.2	The fitted curve of the FT-IR spectrum of GO.	85
Figure 3.3	The fitted curve of the Raman spectrum of GO.	85
Figure 3.4	SEM image of (a) PBTTT/GO composite and, (b) pristine PBTTT FTM film over solid substrate. (c) TEM image of PBTTT/GO composite FTM film over Cu grid. Inset shows the PBTTT/GO composite FTM film at a higher magnification. (d) HR-TEM image of the composite film showing the (010) plane. Inset shows the SAED image of the PBTTT/GO composite FTM film. (e) Fluorescence image (100 x) of PBTTT/GO film formed by FTM technique.	87

List of figures

Figure 3.5	AFM topography, phase image and KPFM image (scan area – 3.5 $\mu\text{m} \times 3.5 \mu\text{m}$) of (a–c) the PBTTT/GO nanocomposite and (d–f) the pristine PBTTT FTM film, respectively.	89
Figure 3.6	GIXD of (a) GO cast from chloroform, (b) PBTTT/GO hybrid, and (c) PBTTT FTM film with grazing angle 0.21°.	90
Figure 3.7	(a) FTIR spectra of (i) PBTTT and (ii) PBTTT/GO, (b) Normalized absorption spectra of PBTTT and PBTTT/GO nanocomposite FTM films over ITO-coated glass substrate	92
Figure 3.8	Cyclic voltammetry of the PBTTT/GO nanocomposite and pure FTM films over ITO-coated glass substrate.	93
Figure 3.9	(a) I_{ds} - V_{ds} output and (b) transfer characteristics of pristine PBTTT thin film.	95
Figure 3.10	(a) I_{ds} - V_{ds} output and (b) transfer characteristics of PBTTT/GO nanocomposite thin film. (c) Schematic of the thin film transistor containing the composite thin film with uniform distribution of GO sheets in a crystalline polymer matrix.	96
Figure 3.11	I_d - V_g transfer characteristics of PBTTT/GO nanocomposite thin film at 10 different places at $V_d = -30 \text{ V}$	97
Figure 4.1	XRD pattern of (a) GO(i) and rGO(ii).(b) HRSEM images of GO(i) and rGO (ii).(c)TEM images of GO(i) and rGO(ii).(d)UV-VIS of GO(i) and rGO (ii).(e)FTIR of GO(i) and rGO(ii).(f)Raman of GO(i) and rGO (ii).	103
Figure 4.2	TEM image of (a)PBTTT and (b-d)PBTTT/rGO composite FTM film over Cu grid. (d) HR-TEM image of composite film showing (010) plane. The SAED picture of the PBTTT/rGO composite FTM film is seen in the inset.	106
Figure 4.3	AFM topography, phase image and KPFM image (scan area 5 $\mu\text{m} \times 5 \mu\text{m}$) of (a-c)PBTTT/GO nanocomposite, and (d-f) pristine PBTTT FTM film.	107
Figure 4.4	Out of plane XRD of PBTTT/rGO and PBTTT FTM film	108
Figure 4.5	(a) Normalized spectral response of PBTTT, and PBTTT/rGO nanocomposite FTM film and (b) FTIR spectra of (i) PBTTT and (ii) PBTTT/rGO.	110
Figure 4.6	CV of PBTTT/rGO nanocomposite, and pure PBTTT FTM film over ITO-coated glass substrate	112

List of figures

Figure 4.7	Output (I_{DS} - V_{DS}) and transfer characteristics (I_{DS} - V_{GS}) of (a,b) pristine PBTTT and (c,d) PBTTT/rGO nanocomposite thin film	114
Figure 4.8	I_{DS} - V_{GS} transfer characteristics of PBTTT/rGO nanocomposite thin film at 10 different places at $V_{DS} = -40$ V	115
Figure 5.1	(a) UV-Vis spectrum of GQDs,(b) Photoluminescence spectrum of GQDs,(c)TEM image of GQDs, where inset is showing corresponding particle size distribution histogram,(d) FTIR spectrum of GQDs,(e) XPS spectrum of C1s of GQDs.	121
Figure 5.2	(a) Powder XRD of PBTTT/GQDs and PBTTT FTM film,(b) TEM image of PBTTT FTM film,(c) TEM image of PBTTT/GQDs composite FTM film, where inset shows the image in higher magnification (d) HR-TEM image of composite film showing (010) plane. The SAED picture of the PBTTT/GQDs composite FTM film is seen in the inset,(e) UV-Vis spectrum of PBTTT, and PBTTT/GQDs nanocomposite FTM film, (f) FTIR spectrum of PBTTT and PBTTT/GQDs (g) CV of PBTTT and PBTTT/GQDs nanocomposite FTM film over ITO coated glass substrate	126
Figure 5.3	Output (I_{DS} - V_{DS}) and transfer characteristics (I_{DS} - V_{GS}) of (a,b) pristine PBTTT and (c,d) PBTTT/GQDs nanocomposite FTM thin film	129
Figure 5.4	I_{DS} - V_{GS} transfer characteristics of PBTTT/GQDs nanocomposite thin film at 10 different places at $V_{DS} = -40$ V	130
Figure 6.1	Characterization of two-dimensional (2D) activated carbon using (a) XRD, (b) Raman (before and after activation) (c) Fourier transform infrared (FTIR) spectroscopies, (d) scanning electron microscopy (SEM), and (e) high-resolution transmission electron microscopy (HR-TEM) image; the inset shows an enlarged view of the TEM image. (f) N_2 adsorption–desorption isotherms; the inset shows the pore size distribution curve	135
Figure 6.2	(a) Study of different pH values using DPV; (b) CV plot of bare and 2D-AC-modified GCE in 5.0 mM $K_3[Fe(CN)_6]/K_4[Fe(CN)_6]$ redox couple in 0.1 M PBS at the scan rate of 50 mV s ⁻¹ ; (c) DPV plot of bare GCE, graphite powder (Gr)-modified GCE, and 2D-AC-modified GCE in 0.1 M PBS at pH 7 in the absence and presence of 76 μ M ROX (the inset shows an enlarged view of the dotted circled area); and (d) the Nyquist plots of (i) bare GCE, (ii) 2D-AC without ROX, and (iii) 2D-AC-modified GCE with 76 μ M ROX	138

List of figures

Figure 6.3	DPV curve (a) and its calibration plot (b) of 2D carbon-modified GCE with successive addition of ROX (0 μM , then 0.76–474 μM) in deoxygenated 0.1 M PBS	140
Figure 6.4	Schematic representation of the reduction of roxarsone on the 2D carbon-modified electrode	141
Figure 6.5	DPV curve and its calibration plot of 2D-AC-modified GCE with successive addition of ROX (5.31–23.55 μM) in deoxygenated 0.1 M PBS (pH 7.0) in human blood serum at a 50 mV s^{-1} scan rate	142
Figure 6.6	DPV curve (a) and its calibration plot (b) of M-AC-modified SPCE with successive addition of ROX (1.89–387.34 μM) in deoxygenated 0.1 M PBS (pH 7.0) at 50 mV s^{-1}	143
Figure 6.7	(a) Reproducibility and (b) storage stability test of the 2D carbon-modified electrode using DPV in the presence of 76 μM ROX in 0.1 M phosphate buffer (pH 7). The inset shows % current retention in the interval of 3 days.	144
Figure 6.8	Interference study using various biological compounds toward ROX in a 10:1 ratio in 0.1 M phosphate buffer (pH 7).	145

List of Tables

Table No.	Table Caption	Page No.
Table 6.1	Comparison of Analytical performance of ROX with other published work	140

LIST OF ABBREVIATIONS

AC	Activated carbon
AFM	Atomic Force Microscopy
Al	Aluminum
Aq.	Aqueous
Au	Gold
BET	Brunauer-Emmet-Teller
CB	Conduction band
CHCl ₃	Chloroform
CNT	Carbon nanotube
CV	Cyclic voltammetry
DPV	Differential pulse voltammetry
DI	Deionised water
EIS	Electrochemical impedance spectroscopy
Eq.	Equation
FESEM	Field emission scanning electron microscopy
Fig.	Figure
FTIR	Fourier transform infrared spectroscopy
FTM	Floating Film Transfer methods
GCE	Glassy carbon electrode
GO	Graphene oxide
GQDs	Graphene quantum dots
Gr	Graphite
HOMO	Highest Occupied Molecular Orbital.
HRSEM	High Resolution Scanning Electron Microscopy
HRTEM	High resolution transmission electron microscopy
ITO	Indium Tin Oxide

LIST OF ABBREVIATIONS

KPFM	Kelvin probe force microscopy
LB	Langmuir Blodgett
LOD	Limit of detection
LOQ	Limit of Quantification
LS	Langmuir Schaefer
LUMO	Lowest Unoccupied Molecular Orbital
MW	Molecular Weight
nm	Nanometer
OFET	Organic Field Effect Transistor
PA	Polyacetylene
PBS	Phosphate buffer solution
PBTTT	Poly(2,5-bis(3-alkylthiophen-2-yl)thieno[3,2-b]thiophene)
P3HT	Poly(3-hexylthiophene)
PPy	Polypyrrole
PQT-12	Poly (3, 3'''- <i>dialkylquarterthiophene</i>)
PT	polythiophene
rGO	reduced Graphene Oxide
ROX	3-nitro-4-hydroxyphenyl arsonic acid
R ²	Regression coefficient value
rr P3AT	regioregular poly (3-aklylthiophene)
SAED	Selected Electron Diffraction pattern
SD	Standard Deviation
Sec	Second
SEM	Scanning Electron Microscopy
S/N	Signal to noise ratio

LIST OF ABBREVIATIONS

SPGE	Screen printed graphite electrode
TEM	Transmission electron microscopy
UV-Vis	Ultraviolet- Visible
XRD	X-ray diffraction
XPS	X-ray photoelectron spectroscopy
d	interplanar spacing
eV	electron volt
θ	theta
ν	scan rate
R	Gas constant
T	Temperature
V	Volt
μA	Microampere
μM	Micromolar
Si	Silicon
SiO ₂	Silicon dioxide
2-D	Two dimensional
3-D	Three dimensional